

Enhanced Multi-sensor Data Fusion Methodology based on Multiple Model Estimation for Integrated Navigation System

Lei Wang* and Shuangxi Li

Abstract: A novel multi-sensor data fusion methodology is presented in this paper with respect to noise with unknown or randomly varying statistics properties and outliers in the SINS/GPS/Odometer integrated navigation system. The proposed methodology combines an adaptive interacting multiple model filtering (AIMM) and federated Kalman algorithm. The former implements dynamic interaction and dynamic change of multiple modes based on the Markov chain process of system models. To achieve the adaptive outlier detection and processing in the measurement signal, modified Kalman filter based on orthogonality of innovation serves as the parallel model filters in the AIMM approach. The advantage of decentralized filter architecture of the latter federated algorithm is flexibility and modularity. It has received considerable attention because of its outstanding fault detection and isolation capability. Experiment results show that the proposed multi-sensor data fusion methodology significantly improves the navigation estimation accuracy and reliability as compared to the federated extend Kalman filter and federated IMM filter approaches.

Keywords: Interacting multiple model, innovation correction, multi-sensor data fusion, SINS/GPS/odometer.

1. INTRODUCTION

Accurate positioning of a moving vehicle is one of the great challenges in the field of navigation. The integrated navigation consisted of global positioning system (GPS), strapdown inertial navigation system (SINS) and odometer is usually adopted for land vehicles [1,2]. Multi-sensor data fusion shows significant advantages in state estimation over single source data. To fuse the information from the above sensors, different approaches can be found in the actual literature [3,4]. Based on Kalman filter, multiple sensors data can be fused in two ways: one is centralized Kalman filter and the other is distributed Kalman filter. The centralized Kalman filter can obtain the optimal state estimate in ideal condition, but the main drawback is the high dimensions of states that may cause the heavy computational load. The distributed Kalman filter is a two-stage data processing technology, which substitutes the original centralized filter with a global filter and several local filters. The Federated Kalman filter developed by Carlson [5] is a special distributed Kalman filter including a process of information sharing and data fusion. A federated filter consists of a distributed filter structure and is divided into parallel sensor-dedicated local Kalman

filters, which process subsets of sensor data. A master filter periodically fuses the local filter estimates according to the least squares criterion, yielding the overall navigation solution.

To achieve good performance from the federated Kalman filter, the stochastic information provided to the local Kalman filters must be accurate. However, GPS is easily subject to abnormal performance. Specifically, signal jamming from nearby radio emitters can cause position error that exceeds several hundreds of meters. Performance degradation may also occur due to both dilution of precision reduction at low altitudes and multipath effects. These GPS measurement errors can cause high measurement noise [6]. Similarly, rough road conditions will cause the change of statistical characteristics of odometer measurement noise. Taking into account the complexity of actual environmental conditions, the stochastic characteristics of noise are sensitive to many factors. So, adaptive method is necessary to accommodate for changes in environmental conditions. The interacting multiple model (IMM) [7,8] has received much attention in recent years due to its unique power and great success in identifying noise with unknown or randomly varying statistics properties, and in decomposing complex

Manuscript received April 1, 2016; revised December 9, 2016; accepted June 24, 2017. Recommended by Associate Editor Chang Kyung Ryoo under the direction of Editor Hyun-Seok Yang. This journal was supported by the Natural Science Foundation of Anhui province (1708085QF146), Talent stabilization project of Anhui Science and Technology University (DQWD201601) and the Foundation of Key Laboratory of Micro-Inertial Instrument and Advanced Navigation Technology, Ministry of Education, China (SEU-MIAN-201701).

Lei Wang and Shuangxi Li are with the School of Electrical and Electronic Engineering, Anhui Science and Technology University, Donghua Road 9 #, Fengyang County, Anhui Province, 233100, China (e-mails: frank_408@163.com, llsx@ahstu.edu.cn).

* Corresponding author.

problems into simpler sub-problems, such as target tracking, image processing, fault detection and integrated navigation, etc. [9–12]. Zang *et al.* [13] have described the IMM technique that can solve the problem of uncertainly noise in the SINS/GPS integrated navigation system. Xu *et al.* [14] have presented an improved interacting multiple model algorithm to estimate the rough value of measurement noise statistical characteristics. The basic idea of IMM approach is to construct a set of possible candidate models for the true plant. A bank of filters run in parallel where each filter is designed using a unique model that may represent the true behavior pattern of the plant.

However, if there are outliers in the measurement signal, the accuracy and stability of all the parallel Kalman filters in IMM algorithm will be affected. As a result, the global estimation by IMM algorithm may be subject to a considerable margin of error. In order to solve this problem, a method of adaptive outlier detection and processing based on orthogonality of innovation in Kalman filter is proposed. The modified Kalman filter is then introduced as parallel filter of IMM algorithm to constitute the AIMM algorithm, which serves as local filter of federated Kalman filtering architecture. The resulted federated AIMM algorithm can overcome the disadvantages of decentralized fusion by combining local decentralized data fusion with global fusion and a two-level structure is formed to improve the accuracy and reliability of integrated navigation systems. The dynamic model of SINS/GPS/odometer integrated systems is developed to describe the system state and observation. A federated estimation fusion method is established for individual integrations of GPS and odometer into SINS to independently obtain the local optimal state estimations of integrated subsystems SINS/GPS and SINS/Odometer. A global optimal estimation fusion theory is studied for fusion of the local optimal estimations to generate the global optimal state estimation of SINS/GPS/Odometer navigation systems. Experimental results are presented to demonstrate the efficacy of the proposed methodology.

The rest of the paper is organized as follows: Section 2 derives theory and structure of the proposed AIMM algorithm. Section 3 describes the data fusion methodology and error model of the integrated navigation system. Section 4 validates the theoretical analyses and illustrates the proposed algorithm using road tests in downtown scenarios and finally. Section 5 gives some concluding remarks.

2. AIMM ALGORITHM BASED ON INNOVATION CORRECTION

For the dynamic state space estimation system, the innovation refers to the deviation of the current observation and its prediction. When the system model in the Kalman filter coincide with the true model, including structure, parameters and noise statistics properties, the innovations

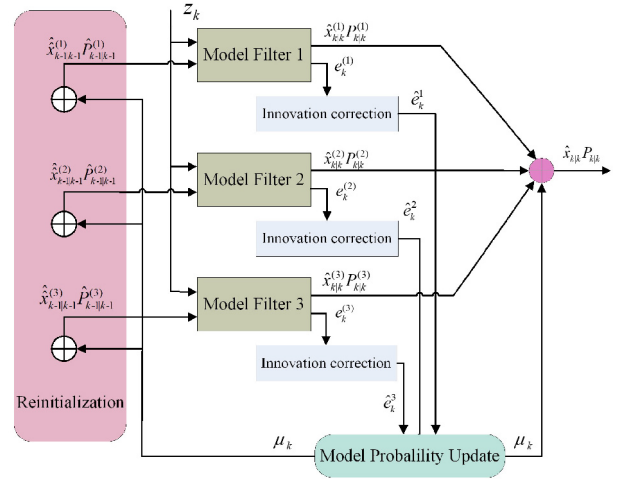


Fig. 1. Structure of the proposed AIMM algorithm ($r = 3$).

will be a Gaussian white noise sequence with zero mean [15, 16]. The consistency of the true model and the filtering model is hidden in the innovations. In the traditional IMM algorithm, the innovations are used to amend the model probabilities. But in most cases, the characteristics of noise are time-varying and hard to get accurately, which may cause wrong correction to the model probabilities and bad performance for the estimation of IMM algorithm. So a process of innovation correction is introduced to incorporate with IMM in this paper. The inputs to the proposed algorithm are the modeled state space and measurement vectors. The AIMM algorithm provides a soft switching among the different inputs. The structure of the AIMM approach is shown in Fig. 1.

2.1. Modified Kalman filter

Consider the following class of single-input and single-output discrete-time systems:

$$\begin{cases} \mathbf{X}_{k+1} = \mathbf{F}_k \mathbf{X}_k + \mathbf{G}_k \mathbf{w}(k), \\ \mathbf{Z}_k = \mathbf{H}_k \mathbf{X}_k + \mathbf{v}_k, \end{cases} \quad (1)$$

where $\mathbf{X}_k \in \mathbb{R}^n$ is the system state; $\mathbf{F}_k \in \mathbb{R}^{n \times n}$ is state transition matrix; $\mathbf{G}_k \in \mathbb{R}^{n \times l}$ is system noise matrix; $\mathbf{Z}_k \in \mathbb{R}^m$ is measurement output; $\mathbf{H}_k \in \mathbb{R}^{m \times n}$ is measurement matrix; $\mathbf{w}_k \in \mathbb{R}^l$ and $\mathbf{v}_k \in \mathbb{R}^m$ are system noise and measurement noise vectors assumed as Gauss white noise with zero mean and independent of each other. The covariance matrices of system noise \mathbf{w}_k and measurement noise \mathbf{v}_k are \mathbf{Q} and \mathbf{R} , respectively.

For system (1), the discrete-time Kalman filter can be described as the following form:

$$\hat{\mathbf{X}}_{k+1|k} = \mathbf{F}_{k+1|k} \hat{\mathbf{X}}_k, \quad (2)$$

$$\mathbf{P}_{k+1|k} = \mathbf{F}_{k+1|k} \mathbf{P}_k \mathbf{F}_{k+1|k}^T + \mathbf{G}_k \mathbf{Q}_k \mathbf{G}_k^T, \quad (3)$$

$$\mathbf{e}_{k+1} = \mathbf{Z}_{k+1} - \mathbf{H}_{k+1} \hat{\mathbf{X}}_{k+1|k}, \quad (4)$$

$$\mathbf{K}_{k+1} = \mathbf{P}_{k+1|k} \mathbf{H}_{k+1}^T (\mathbf{H}_{k+1} \mathbf{P}_{k+1|k} \mathbf{H}_{k+1}^T + \mathbf{R}_{k+1})^{-1}, \quad (5)$$

$$\hat{\mathbf{X}}_{k+1} = \hat{\mathbf{X}}_{k+1|k} + \mathbf{K}_{k+1} \mathbf{e}_{k+1}, \quad (6)$$

$$\mathbf{P}_{k+1} = (\mathbf{I} - \mathbf{K}_{k+1} \mathbf{H}_{k+1}) \mathbf{P}_{k+1|k} (\mathbf{I} - \mathbf{K}_{k+1} \mathbf{H}_{k+1})^T + \mathbf{K}_{k+1} \mathbf{R}_{k+1} \mathbf{K}_{k+1}^T, \quad (7)$$

where \mathbf{e}_{k+1} in (4) is called the innovation sequence of Kalman filter and its covariance matrix \mathbf{s}_{k+1} can be calculated by

$$\mathbf{s}_{k+1} = E(\mathbf{e}_{k+1} \mathbf{e}_{k+1}^T) = \mathbf{H}_{k+1} \mathbf{P}_{k+1|k} \mathbf{H}_{k+1}^T + \mathbf{R}_{k+1}. \quad (8)$$

It can be proved that the innovation \mathbf{e}_{k+1} is an independent identically distributed sequence and has the property of orthogonality [17]:

$$E\{\hat{\mathbf{e}}_{k+1} \mathbf{Z}_m\} = 0, \quad m < k + 1. \quad (9)$$

If there are outliers in the measurement sequence \mathbf{Z}_{k+1} , the orthogonality of innovation \mathbf{e}_{k+1} will be disrupted. This will be useful for the outlier detection. Suppose $\hat{\mathbf{Z}}_{k+1}$ is the optimal estimation of \mathbf{Z}_{k+1} , a symbol Φ_{k+1} is defined as

$$\begin{aligned} \Phi_{k+1} &= E(\mathbf{Z}_{k+1} \mathbf{Z}_{k+1}^T) \\ &= E(\mathbf{e}_{k+1} \mathbf{e}_{k+1}^T) + E(\hat{\mathbf{Z}}_{k+1} \hat{\mathbf{Z}}_{k+1}^T). \end{aligned} \quad (10)$$

Since the optimal estimation $\hat{\mathbf{Z}}_k$ can be denoted by

$$\hat{\mathbf{Z}}_{k+1} = \mathbf{H}_{k+1} \hat{\mathbf{X}}_{k+1|k}. \quad (11)$$

Put (8) and (11) into (10),

$$\begin{aligned} \Phi_{k+1} &= E[\mathbf{Z}_{k+1} \mathbf{Z}_{k+1}^T] = \mathbf{H}_{k+1} \mathbf{P}_{k+1|k} \mathbf{H}_{k+1}^T + \mathbf{R}_{k+1} \\ &\quad + \mathbf{H}_{k+1} \hat{\mathbf{X}}_{k+1|k} \hat{\mathbf{X}}_{k+1|k}^T \mathbf{H}_{k+1}^T. \end{aligned} \quad (12)$$

For the sake of convenience in writing, a symbol Θ_{k+1} is defined as

$$\begin{aligned} \Theta_{k+1} &= \mathbf{H}_{k+1} \mathbf{P}_{k+1|k} \mathbf{H}_{k+1}^T + \mathbf{R}_{k+1} \\ &\quad + \mathbf{H}_{k+1} \mathbf{X}_{k+1|k} \mathbf{X}_{k+1|k}^T \mathbf{H}_{k+1}^T. \end{aligned} \quad (13)$$

Then a judgment criterion if there are outliers in the measurement data can be got by

$$\Phi_{(i,i)k+1} \in [\Theta_{(i,i)k+1} - \varepsilon, \Theta_{(i,i)k+1} + \varepsilon], \quad (14)$$

where $\Phi_{(i,j)k+1}$ and $\Theta_{(i,j)k+1}$ denote the diagonal elements of $\Phi_{(i,j)k+1}$ and $\Theta_{(i,j)k+1}$, respectively. If equation (14) is valid, it can be considered that there are no outliers in the measurement. Otherwise, there are outliers in the measurement. Considering the calculation error, a perturbation ε is introduced and it can be selected according the actual situation.

In order to reduce the state estimation error caused by outliers, an amendment method is proposed to replace the predicting equation (6) in Kalman filter.

$$\hat{\mathbf{X}}_{k+1} = \hat{\mathbf{X}}_{k+1|k} + \mathbf{K}_{k+1} (\mathbf{B}_{k+1} - \mathbf{H}_{k+1} \hat{\mathbf{X}}_{k+1|k}), \quad (15)$$

where

$$\mathbf{B}_{k+1} = [\mathbf{Z}_{(1)k+1} f_1(\chi_1) \quad \mathbf{Z}_{(2)k+1} f_2(\chi_2) \quad \cdots \quad \mathbf{Z}_{(m)k+1} f_m(\chi_m)]^T, \quad (16)$$

where $f_m(\chi_m)$, ($i = 1, 2, \dots, m$) is an activation function and it must have the following properties:

- 1) when $\chi_i \rightarrow \infty$, $f_i(\chi_i) \rightarrow 0$;
- 2) when $\chi_i < C$ or $\chi_i \geq C$, $f_i(\chi_i)$ is a constant, where C is threshold;
- 3) $f_i(\chi_i)$ is monotonic decline and continuously differentiable.

In our work, a piecewise smooth function is adopted and its specific form is as follows:

$$f_i(\chi_i) = \begin{cases} 1, & \chi_i \leq d_i, \\ d_i/\chi_i, & \chi_i > d_i, \end{cases} \quad (17)$$

where

$$\chi_i = \sqrt{\Phi_{(i,i)k+1}}, \quad d_i = \sqrt{\Theta_{(i,i)k+1} + \varepsilon_i}, \quad i = 1, 2, \dots, m. \quad (18)$$

As can be seen from the above process, the measurement \mathbf{Z}_{k+1} is detected by (14). If outliers exist in \mathbf{Z}_{k+1} , $\chi_i > d_i$ and $f_i(\chi_i) = d_i/\chi_i < 1$, module of the measurement \mathbf{Z}_{k+1} will be reduced by multiplying with the function $f_i(\chi_i)$ in the amendment predicting equation (15). On the contrary, if there are no outliers in the measurement, module of \mathbf{Z}_{k+1} will keep for $f_i(\chi_i) = d_i/\chi_i = 1$. In addition, the perturbation ε can be adjusted to meet different kinds of application requirements.

2.2. AIMM algorithm

Suppose the model set is \mathbf{M} with r models, the effective model at time k is m_k , the dynamic system can be described as

$$\begin{cases} \mathbf{X}_{k+1} = \mathbf{F}_k(m_k) \mathbf{X}_k + \mathbf{G}_k \mathbf{w}_k(m_k), \\ \mathbf{Z}_k = \mathbf{H}_k(m_k) \mathbf{X}_k + \mathbf{v}_k(m_k), \end{cases} \quad (19)$$

where \mathbf{X}_k is the state vector, \mathbf{Z}_k is the observation vector, \mathbf{G}_k is the process matrix, \mathbf{H}_k is the measurement matrix, \mathbf{w}_k and \mathbf{v}_k are the process noise and observation noise sequence respectively. The initial Markov transition probability π_{ji} can be denoted by:

$$\pi_{ji} = P\{m_{k+1}^j | m_k^i\}, \quad m_k^i, m_{k+1}^j \in \mathbf{M}. \quad (20)$$

As can be seen from Fig. 1, the proposed AIMM algorithm consists of r interacting filters operating in parallel and r is set as 3 in our work. One cycle of the algorithm consists of the following steps:

1) Model re-initialization. At time $k + 1$, the initial condition of the j th ($1 \leq j \leq r$) model matched filter is obtained by mixing the state estimates of all filters at the

previous time. The initial model transition probability $\boldsymbol{\mu}_{k|k}^j$ is

$$\boldsymbol{\mu}_{k|k}^j = \frac{\pi_{ji} \boldsymbol{\mu}_k^i}{\sum_{i=1}^r \pi_{ji} \boldsymbol{\mu}_k^i}, \quad (21)$$

where $\boldsymbol{\mu}_k^i$ is the probability of model i at time k . The mixing state estimation $\hat{\mathbf{X}}_k^j$ and its estimation error covariance \mathbf{P}_k^j are given by

$$\hat{\mathbf{X}}_k^j = \sum_{i=1}^r \boldsymbol{\mu}_{k|k}^j \hat{\mathbf{X}}_k^i, \quad (22)$$

$$\mathbf{P}_k^j = \sum_{i=1}^r \hat{\boldsymbol{\mu}}_{k|k}^j \left[\mathbf{P}_{k|k}^i + \left(\hat{\mathbf{X}}_k^j - \hat{\mathbf{X}}_{k|k}^i \right) \left(\hat{\mathbf{X}}_k^j - \hat{\mathbf{X}}_{k|k}^i \right)^T \right], \quad (23)$$

where $\hat{\mathbf{X}}_{k|k}^i$ and $\mathbf{P}_{k|k}^i$ are respectively the estimates of state and its estimation error covariance of model i at time k .

2) Matched model filtering. This step performs for each model an individual filtering. The modified Kalman filter is used as the matched model filter in the proposed algorithm. For the j th model filter, detailed steps are illustrated as follows:

$$\hat{\mathbf{X}}_{k+1|k}^j = \mathbf{F}_{k+1|k}^j \hat{\mathbf{X}}_{k|k}^j, \quad (24)$$

$$\mathbf{P}_{k+1|k}^j = \mathbf{F}_{k+1|k}^j \mathbf{P}_k^j \left(\mathbf{F}_{k+1|k}^j \right)^T + \mathbf{G}_k^j \mathbf{Q}_k^j \left(\mathbf{G}_k^j \right)^T, \quad (25)$$

$$\mathbf{e}_{k+1}^j = \mathbf{Z}_{k+1}^j - \mathbf{H}_{k+1}^j \hat{\mathbf{X}}_{k+1|k}^j, \quad (26)$$

$$\mathbf{K}_{k+1}^j = \mathbf{P}_{k+1|k}^j \left(\mathbf{H}_{k+1}^j \right)^T \times \left[\mathbf{H}_{k+1}^j \mathbf{P}_{k+1|k}^j \left(\mathbf{H}_{k+1}^j \right)^T + \mathbf{R}_{k+1}^j \right]^{-1}, \quad (27)$$

$$\hat{\mathbf{X}}_{k+1}^j = \hat{\mathbf{X}}_{k+1|k}^j + \mathbf{K}_{k+1}^j \left(\mathbf{B}_{k+1}^j - \mathbf{H}_{k+1}^j \hat{\mathbf{X}}_{k+1|k}^j \right), \quad (28)$$

$$\mathbf{P}_{k+1}^j = \left(\mathbf{I} - \mathbf{K}_{k+1}^j \mathbf{H}_{k+1}^j \right) \mathbf{P}_{k+1|k}^j \left(\mathbf{I} - \mathbf{K}_{k+1}^j \mathbf{H}_{k+1}^j \right)^T + \mathbf{K}_{k+1}^j \mathbf{R}_{k+1}^j \left(\mathbf{K}_{k+1}^j \right)^T. \quad (29)$$

It can be seen that amendment predicting equation is used to replace equation (6) in Kalman filter. Calculation of \mathbf{B}_{k+1}^j in (28) can refer to (16), (17) and (18). Then the state estimation $\hat{\mathbf{X}}_{k+1}^j$ and its corresponding estimation covariance \mathbf{P}_{k+1}^j can be acquired.

3) Innovation correction. The corrected innovation $\hat{\mathbf{e}}_{k+1}^j$ and its covariance \mathbf{S}_{k+1}^j can be calculated by:

$$\hat{\mathbf{e}}_{k+1}^j = \mathbf{B}_{k+1}^j - \mathbf{H}_{k+1}^j \hat{\mathbf{X}}_{k+1|k}^j, \quad (30)$$

$$\mathbf{S}_{k+1}^j = \mathbf{H}_{k+1}^j \mathbf{P}_{k+1|k}^j \left(\mathbf{H}_{k+1}^j \right)^T + \mathbf{R}_{k+1}^j. \quad (31)$$

Compare to (26), it can be seen that the new innovation equation (30) can reduce the affection of outliers in measurement signal. The new innovation $\hat{\mathbf{e}}_{k+1}^j$ can make the

calculation of the subsequent model probability more precise and decrease the sensitivity of probabilistic weightings to measurement noise.

4) Model probability update. The likelihood function $\boldsymbol{\Lambda}_{k+1}^j$ of the model m_j can be simplified as

$$\boldsymbol{\Lambda}_{k+1}^j = N \left[\hat{\mathbf{e}}_{k+1}^j; \mathbf{0}, \mathbf{S}_{k+1}^j \right] = \left[(2\pi)^n \left| \mathbf{S}_{k+1}^j \right| \right]^{-1/2} \times \exp \left\{ -\frac{1}{2} \left(\hat{\mathbf{e}}_{k+1}^j \right)^T \left(\mathbf{S}_{k+1}^j \right)^{-1} \hat{\mathbf{e}}_{k+1}^j \right\}, \quad (32)$$

where n is the dimension of state, then the multiple model probability can be updated as

$$\boldsymbol{\mu}_{k+1|k}^j = P \left\{ m_{k+1}^j | \mathbf{Z}_{k+1}^j \right\} = \frac{\boldsymbol{\Lambda}_{k+1}^j \sum_{j=1}^r \pi_{ji} \boldsymbol{\mu}_{k|k}^j}{\sum_{i=1}^r \left[\boldsymbol{\Lambda}_{k+1}^i \sum_{j=1}^r \pi_{ji} \boldsymbol{\mu}_{k|k}^j \right]}. \quad (33)$$

5) Output combination. The filter estimation based on each model is weighted and combined to generate the resulting filter state estimation. This is only done for output purpose and further usage in data association. It is not part of the algorithm recursions.

$$\hat{\mathbf{X}}_{k+1} = \sum_{j=1}^r \boldsymbol{\mu}_{k+1|k}^j \hat{\mathbf{X}}_{k+1}^j, \quad (34)$$

$$\mathbf{P}_{k+1} = \sum_{j=1}^r \boldsymbol{\mu}_{k+1|k}^j \times \left[\mathbf{P}_k + \left(\hat{\mathbf{X}}_{k+1}^j - \hat{\mathbf{X}}_{k+1} \right) \left(\hat{\mathbf{X}}_{k+1}^j - \hat{\mathbf{X}}_{k+1} \right)^T \right]. \quad (35)$$

3. SINS/GPS/ODOMETER INTEGRATED NAVIGATION SYSTEM

3.1. Data fusion methodology

SINS is a precision instrumentation system, which provides the geographical position, velocity, and attitude of a vehicle by using inertial sensors, such as gyroscopes and accelerometers. In the system the accelerations measured by accelerometers and the angular velocities by gyroscopes are integrated without external aids. Through the integration linear velocity, position, and attitude can be obtained. Therefore, it can provide navigation solution continually. However, the measurement errors in accelerometers and gyroscopes will be integrated together with the true values, and then they accumulate in position solution without limit. GPS is a satellite-based radio navigation system, which provides highly accurate position data of a vehicle to users. For position calculation, generally at least four satellites must be visible. However, in an urban area, the number of visible satellites is often less than four due to tall building and trees. Therefore, with only a GPS receiver, continuous navigation is impossible

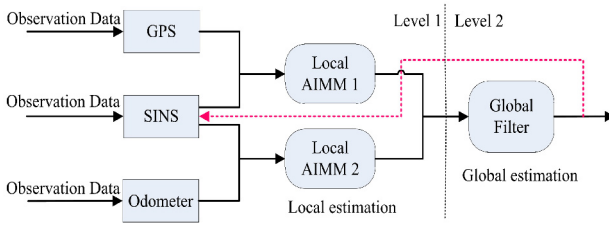


Fig. 2. Structure of the multi-sensor data fusion methodology.

[18]. Odometer is an instrument which can provide vehicle with velocity relative to land. Different from inertial navigation system, the velocity is measured directly, so it is bounded and of high accuracy. From the point of long-term evolution, velocity error is far less than the inertial navigation system. The SINS/GPS/Odometer integrated system incorporates the characteristics of each navigation system. To be specific, SINS provides data with good short-term stability while the GPS and odometer provide data with good long-term stability. It integrates the output of the inertial measurement unit (IMU) at more frequent periods and if the external information by GPS or odometer is available at some instant, it combines those through multi-sensor data fusion method.

To integrate the subsystems GPS and odometer into the main system SINS, a multi-sensor data fusion methodology is established based on federated AIMM filter. Fig. 2 depicts the structure of the federated filter, in which no-reset mode is adopted. The observation information of the integrated navigation system includes the GPS position P_{GPS} and velocity V_{GPS} , the SINS position P_{INS} and velocity V_{INS} , and the velocity V_{OD} measured in body frame by odometer. Subsystems GPS and odometer independently observe the output of SINS. The two local filters estimate the state of SINS according to the observed data. Combining the local decentralized fusion with global optimal fusion, a two-level structure fusion methodology is formed to achieve the accuracy and reliability of the integrated system from the overall of the point. At the first level, GPS and odometer are integrated with SINS by two local AIMM filters respectively. This level is a parallel process of decentralized estimation based on the observation space. At the second level, the local optimal estimations generated from these two local filters are fused together to generate the global optimal state estimation of the SINS/GPS/Odometer integrated navigation system.

SINS is used to establish the inertia navigation model. Set the Earth-centered inertial (ECI) frame as the inertial frame (i), the East-North-Up (ENU) geography coordinate as the local navigation frame (n), and the Right-Front-UP (RFU) frame as the body-fixed frame (b), clearer definition can be found in reference [19]. The error model of SINS/GPS/Odometer integrated navigation system can be derived according from the frames defined above.

3.2. SINS/GPS loosely coupled system

3.2.1 System error model

Assume the strapdown inertial navigation attitude error angle $\boldsymbol{\varphi}$ are small angles, and ignore the earth gravity model error, the linear approximation of the strapdown inertial navigation error equation can be obtained [20]. The attitude error equation is given by

$$\dot{\boldsymbol{\varphi}} = -\boldsymbol{\omega}_{in}^n \times \boldsymbol{\varphi} + \delta\boldsymbol{\omega}_{in}^n - \delta\boldsymbol{\omega}_{ib}^n. \quad (36)$$

The speed error equation is:

$$\begin{aligned} \delta\dot{\mathbf{V}}^n = & \mathbf{f}^n \times \boldsymbol{\varphi} - (2\boldsymbol{\omega}_{ie}^n + \boldsymbol{\omega}_{en}^n) \times \delta\mathbf{V}^n \\ & + \dot{\mathbf{V}}^n \times (2\delta\boldsymbol{\omega}_{ie}^n + \delta\boldsymbol{\omega}_{en}^n + \delta\mathbf{f}^n). \end{aligned} \quad (37)$$

The SINS distance increment is

$$\begin{aligned} \delta\mathbf{P} = & \begin{bmatrix} \delta\dot{L} \\ \delta\dot{\lambda} \\ \delta\dot{h} \end{bmatrix} \\ = & \begin{bmatrix} \frac{1}{R_M+h} \delta v_N^n - \frac{v_N^n}{(R_M+h)^2} \delta h \\ \frac{\sec L}{R_N+h} \delta v_E^n + \frac{v_E^n \sec L \tan L}{R_N+h} \delta L - \frac{v_E^n \sec L}{(R_N+h)^2} \delta h \\ \delta v_U^n \end{bmatrix}, \end{aligned} \quad (38)$$

where $[\boldsymbol{\varphi}^T \ \delta\mathbf{V}^{nT} \ \delta\mathbf{P}^T]^T$ represent misalignment angle, velocity error and position error in navigation frame respectively, $\delta\mathbf{V} = [\delta v_E^n \ \delta v_N^n \ \delta v_U^n]^T$ represent velocity error in the navigation frame, and the subscript E , N and U represent east, north and upward axis projections. The scale bias and the installation error of gyros and accelerometers are ignored. The accelerometer error consists of white Gaussian noise and the accelerometer bias error, which is assumed as a random constant. The gyroscope error consists of white Gaussian noise and the gyroscope bias error, which is assumed as a random constant. The error equation for the SINS is given in (39):

$$\mathbf{x}_{INS}(k+1) = \mathbf{F}_{INS}(k)\mathbf{x}_{INS}(k) + \mathbf{G}_{INS}(k)\mathbf{w}(k), \quad (39)$$

where $\mathbf{x}_{INS}(k)$ is the state vector of the system, $\mathbf{F}_{INS}(k)$ is the system vector matrix, $\mathbf{w}(k)$ is system noise and $\mathbf{G}_{INS}(k)$ is the noise coefficient matrix. \mathbf{x}_{INS} is defined as

$$\mathbf{x}_{INS} = [\boldsymbol{\varphi}^T \ \delta\mathbf{V}^{nT} \ \delta\mathbf{P}^T \ \boldsymbol{\varepsilon}^{bT} \ \nabla^{bT}]^T,$$

where $\boldsymbol{\varepsilon}$ is gyroscope bias and ∇ is accelerometer bias.

3.2.2 Measurement error model

The first local filter is SINS/GPS loosely coupled system. The error propagation model of the SINS/GPS loosely coupled system can be formed from the differential equations of the navigation error [21, 22]. The measurement error model can be determined from the GPS position information ($[L_{GPS} \ \lambda_{GPS} \ h_{GPS}]^T$) obtained from the

GPS receiver and the navigation solutions obtained from the SINS ($[\lambda_{SINS} \lambda_{SINS} h_{SINS}]^T$). A time delay Δt is assumed to exist in addition to the GPS position information to obtain the measurement error model. The ignored term can be considered as measurement noise.

$$\begin{aligned} \mathbf{z}_1(t) &= \begin{bmatrix} [L_{SINS}(t) - L_{GPS}(t - \Delta t)](R_m + h_{SINS}) \\ [\lambda_{SINS}(t) - \lambda_{GPS}(t - \Delta t)](R_m + h_{SINS}) \cos(L_{SINS}) \\ -[h_{SINS} - h_{GPS}(t - \Delta t)] \end{bmatrix} \\ &= \begin{bmatrix} \delta p_E(t) + v_{GPSE}(t)\Delta t + p_{mE}(t) \\ \delta p_N(t) + v_{GPSN}(t)\Delta t + p_{mN}(t) \\ \delta p_U(t) + v_{GPSU}(t)\Delta t + p_{mU}(t) \end{bmatrix}, \end{aligned} \quad (40)$$

where ($[v_{GPSE} \ v_{GPSN} \ v_{GPSU}]^T$) is the velocity provided by GPS, and ($[p_{mE} \ p_{mN} \ p_{mU}]^T$) is the measurement noise. Velocity values calculated from INS can replace GPS velocity values when they are not available from the receiver.

3.3. SINS/Odometer integration system

The second local filter contains SINS and odometer, which constitute a dead-reckoning (DR) system. Velocity output by IMU and odometer is utilized to calculate the relative location of the vehicle. Odometer outputs distance increment during a small period of the vehicle. The dead-reckoning algorithm contains position updating and attitude updating. Suppose the odometer frame (m) coordinates with the vehicle body frame (b), then the velocity of the vehicle can be obtained from the output of the odometer

$$\mathbf{v}_D^n(k) = \mathbf{C}_{Db}^n(k) [0 \ \Delta S(k)/T_D \ 0]^T, \quad (41)$$

where $\mathbf{v}_D^n(k)$ is the velocity vector at time t_k ; $\mathbf{C}_{Db}^n(k)$ is the attitude matrix from body frame to the navigation frame at time t_k ; $\Delta S(k)$ is the odometer distance increment during the sampling period and T_D is the odometer output sampling time.

Take the odometer scale factor error and the attitude matrix error into consideration, the actual vehicle velocity $\hat{\mathbf{v}}_D^n$ can be written as follows:

$$\begin{aligned} \hat{\mathbf{v}}_D^n &= \hat{\mathbf{C}}_{Db}^n \hat{\mathbf{v}}_D^b = \mathbf{C}_n^n \mathbf{C}_{Db}^n (1 + \delta k_D) \mathbf{v}_D^b \\ &= (\mathbf{I} - (\phi_D \times)) \mathbf{C}_{Db}^n (1 + \delta k_D) \mathbf{v}_D^b, \end{aligned} \quad (42)$$

where $\hat{\mathbf{C}}_{Db}^n$ is the attitude matrix determined by the dead-reckoning updating; δk_D denotes the error of the odometer scale factor and $(\phi_D \times)$ is the skew symmetric matrix of attitude error in navigation frame. Expand (42) and eliminate the products of error quantities yield

$$\hat{\mathbf{v}}_D^n = \mathbf{v}_D^n + \delta k_D \mathbf{v}_D^b - (\phi_D \times) \mathbf{v}_D^b, \quad (43)$$

where $\mathbf{v}_D^n = \mathbf{C}_{Db}^n [0 \ \mathbf{v}_D \ 0]^T$, and \mathbf{v}_D is the vehicle velocity in the body frame. Subtract \mathbf{v}_D^n from both sides of (43) yields

$$\delta \mathbf{v}_D^n = \delta k_D \mathbf{v}_D^n - (\phi_D \times) \mathbf{v}_D^n, \quad (44)$$

where $\delta \mathbf{v}_D^n$ denotes $\hat{\mathbf{v}}_D^n - \mathbf{v}_D^n$.

The position updating algorithm is of the same form as that of the SINS position algorithm, and its discrete form is given as follows:

$$\begin{cases} L_D(k) = L_D(k-1) + \frac{\Delta S_{DN}(k)}{R_M + h_D(k)}, \\ \lambda_D(k) = \lambda_D(k-1) + \frac{\Delta S_{DE}(k) \sec L_D(k-1)}{R_N + h_D(k-1)}, \\ h_D(k) = h_D(k-1) + \Delta S_{DU}(k), \end{cases} \quad (45)$$

where L_D , λ_D and h_D are the dead-reckoning latitude, longitude and altitude; ΔS_{DE} , ΔS_{DN} and ΔS_{DU} are the odometer distance increment in the east, north and upward, respectively. The position error equation of the odometer dead-reckoning system is as follows:

$$\delta \dot{\mathbf{p}}_D = \mathbf{M}_{D1}(\mathbf{v}_D^n \times) \phi_D + \mathbf{M}_{D2} \delta \mathbf{p}_D + \mathbf{M}_{D1} \mathbf{v}_D^n \delta k_D, \quad (46)$$

where

$$\begin{aligned} \mathbf{v}_D^n &= [v_{DE} \ v_{DN} \ v_{DU}]^T, \\ \delta \mathbf{p}_D &= [\delta L_D \ \delta \lambda_D \ \delta h_D]^T. \end{aligned}$$

\mathbf{M}_{D1} and \mathbf{M}_{D2} are respectively given by

$$\begin{aligned} \mathbf{M}_{D1} &= \begin{bmatrix} 0 & 1/(R_M + h_D) & 0 \\ \sec L_D/(R_N + h_D) & 0 & 0 \\ 0 & 0 & 1 \end{bmatrix}, \\ \mathbf{M}_{D2} &= \begin{bmatrix} 0 \\ v_{DE} \sec L_D \tan L_D/(R_N + h_D) \\ 0 \\ 0 & -v_{DN}/(R_M + h_D)^2 \\ 0 & -v_{DE} \sec L_D/(R_N + h_D)^2 \\ 0 & 0 \end{bmatrix}. \end{aligned}$$

The attitude error equation can be written as

$$\begin{aligned} \dot{\phi}_D &= [\mathbf{M}_{D3}(\mathbf{v}_D^n \times) - (\boldsymbol{\omega}_{in}^n \times)] \phi_D \\ &+ \mathbf{M}_{D4} \delta \mathbf{p}_D + \mathbf{M}_{D3} \mathbf{v}_D^n \delta k_D - \mathbf{C}_{Db}^n \boldsymbol{\epsilon}^b, \end{aligned} \quad (47)$$

where $\boldsymbol{\epsilon}^b$ is the gyro drift rate vector; \mathbf{M}_{D3} and \mathbf{M}_{D4} are given by

$$\begin{aligned} \mathbf{M}_{D3} &= \begin{bmatrix} 0 & -1/(R_M + h_D) & 0 \\ 1/(R_N + h_D) & 0 & 0 \\ \tan L_D/(R_N + h_D) & 0 & 1 \end{bmatrix}, \\ \mathbf{M}_{D4} &= \begin{bmatrix} 0 \\ -\boldsymbol{\omega}_{ie} \sin L_D \\ \boldsymbol{\omega}_{ie} \cos L_D + v_{DE} \sec^2 L_D/(R_N + h_D) \\ 0 & v_{DN}/(R_M + h_D)^2 \\ 0 & -v_{DE}/(R_N + h_D)^2 \\ 0 & -v_{DE} \tan L_D/(R_N + h_D)^2 \end{bmatrix}. \end{aligned}$$

As the dead-reckoning error equations given above and the SINS error equation in Section 3.2.1, the state model

can be written in matrix form. The state and measurement model can be given in matrix form by

$$\begin{cases} \dot{\mathbf{X}}_2(t) = \mathbf{F}_2(t)\mathbf{X}_2(t) + \mathbf{W}_2(t), \\ \mathbf{Z}_2(t) = \mathbf{H}_2(t) + \mathbf{V}_2(t), \end{cases} \quad (48)$$

where $\mathbf{X}_2 = [\delta\mathbf{p}^T \ \delta\mathbf{v}^{n^T} \ \boldsymbol{\varphi}^T \ \boldsymbol{\varepsilon}^{b^T} \ \nabla^{b^T} \ \delta\mathbf{p}_D^T \ \boldsymbol{\varphi}_D^T \ \delta k_D]^T$ is the state vector, $\delta\mathbf{P}$, $\delta\mathbf{V}$ and $\boldsymbol{\varphi}$ are the estimated position error, velocity error and attitude error of SINS, respectively; $\boldsymbol{\varepsilon}^b$ is gyroscope bias and ∇^b is accelerometer bias denoted in the b -frame; $\delta\mathbf{p}_D^T$, $\boldsymbol{\varphi}_D^T$ are the dead-reckoning position error and attitude error vectors; δk_D denotes the error of the odometer scale factor. $\mathbf{W}_2(t)$ is the processing noise vector; $\mathbf{F}_2(t)$ and $\mathbf{H}_2(t)$ are the state transition matrix and measurement matrix. The observations $\mathbf{Z}_2 = [v_{SE} - v_{DE} \ v_{SN} - v_{DN} \ v_{SU} - v_{DU}]^T$ is the deviation of velocity between SINS and the odometer dead-reckoning, where v_{SE} , v_{SN} , v_{SU} and v_{DE} , v_{DN} , v_{DU} are the velocity vectors of SINS and odometer dead-reckoning on navigation frame, respectively, the subscript E , N , U represent east, north and upward axis projections.

3.4. Global fusion algorithm

After completing the computations of the two parallel-processing local AIMM filters, two local optimal state estimations $\hat{\mathbf{x}}_i(k)$ ($i = 1, 2$) can be obtained and further fused by the global filter. In the global filter, we compute a weighted combination of updated state estimates produced by the two local filters yielding a final estimate $\hat{\mathbf{x}}_g(k)$. The weights are chosen according to the error variances $P_i(k)$ ($i=1, 2$) of the two local filters.

$$\hat{\mathbf{x}}_g(k) = P_g(k) \sum_{i=1}^2 P_i^{-1}(k) \hat{\mathbf{x}}_i(k), \quad (49)$$

$$P_g(k) = \left(\sum_{i=1}^2 P_i^{-1}(k) \right)^{-1}. \quad (50)$$

For the no-reset mode federated Kalman filter, the global filter retains none of the fused information, while the local filters collectively retain all of the local information. This no-reset design is highly fault tolerant and, therefore, provides excellent performance for failure detection and isolation because the local filters operate independently of each other. While the GPS signal is available, the global fusion is used to calibrate the IMU and the odometer. When there is GPS signal failure, the first local filter is disabled and pure inertial navigation assisted by odometer is performed till the GPS signal is once again available.

4. EXPERIMENTS AND RESULTS

A field test has been carried out to evaluate the proposed scheme in terms of its efficacy at the proposed integrated navigation systems shown in Fig. 3.



Fig. 3. Experimental vehicle system.

A low-cost IMU and navigation grade SINS/GPS were mounted in the centre of vehicle. The navigation grade SINS/GPS, an integrated navigation system consisting of GPS receiver and a navigation grade IMU, was used to provide precise reference solution. The test GPS antennae with receiver were mounted on the roof of vehicle. Optical odometer was mounted at the back of the vehicle. The raw inertial data from the low-cost IMU were collected at 200 Hz for integration process. Velocity measurement from odometer, position and velocity measurement from test GPS and navigation solution position, velocity and attitude from reference systems were also stored in the file at 1 Hz for post processing and comparison purpose. The raw inertial data was collected from low-cost IMU is post processed in MATLAB environment. A road test trajectory was carried out using the setup described above in downtown Beijing. It had a lot of degraded GPS performance because of either severe signal reflection without a direct line of sight or complete blockage. In the trajectory the vehicle undergoes consecutive turns, accelerations and decelerations. In this paper, the federated extended Kalman filter (EKF) and federated IMM algorithm described in [6, 13, 23] were compared with the proposed federated AIMM methodology for the road test trajectories.

To identify noise with unknown or randomly varying statistics properties in the actual situation, selection of process noise covariance matrix, measurement noise matrix, model transition probability is crucial. For each of the two local AIMM filters in the federated filter, the effective models change among three models based on the Markov transition matrix. The transition values are obtained on the basis of statistics on the system evolution. The initial Markov transition probability π_{ji} is described as follows:

$$\pi_{ji} = \begin{cases} 0.95, & i = j, \\ (1 - 0.95)/2, & i \neq j. \end{cases} \quad (i, j = 1, 2, 3).$$

In the federated filter, the process noise covariance matrices \mathbf{Q}_1 and \mathbf{Q}_2 are regarded as constant. The measurement noise matrices \mathbf{R}_1 and \mathbf{R}_2 are assumed variables in the dynamic system. In the SINS/GPS local filter, the initial measurement noise matrix of is set as $\mathbf{R}_1 = \text{diag} [10 \text{ m} \ 10 \text{ m}]^2$ and the measurement noise

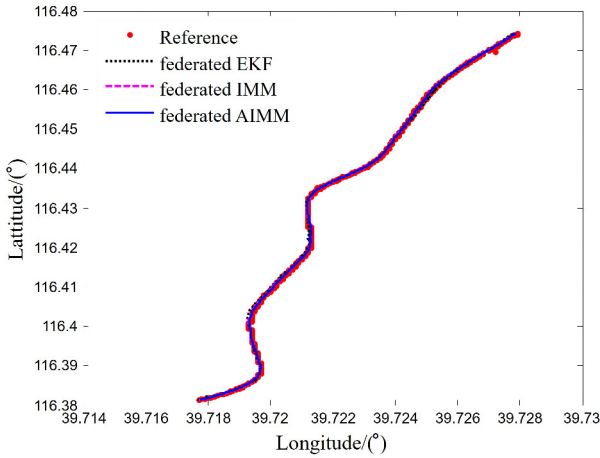


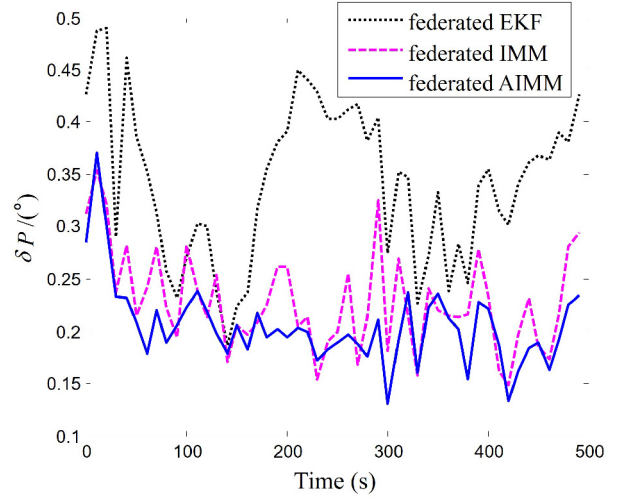
Fig. 4. Trajectory of the test vehicle.

matrices in the three parallel filters are set as \mathbf{R}_1 , $9\mathbf{R}_1$ and $25\mathbf{R}_1$, respectively. In the SINS/Odometer local filter, the initial measurement noise matrix of is set as $\mathbf{R}_2 = \text{diag} [0.05 \text{ m/s} \quad 0.05 \text{ m/s}]^2$ and the measurement noise matrices in the three parallel filters are set as \mathbf{R}_2 , $4\mathbf{R}_2$ and $8\mathbf{R}_2$, respectively. To compare with the federated IMM filter, the same model set is selected for federated AIMM method. In the federated EKF, the measurement noise matrices of the two filters are set as \mathbf{R}_1 and \mathbf{R}_2 .

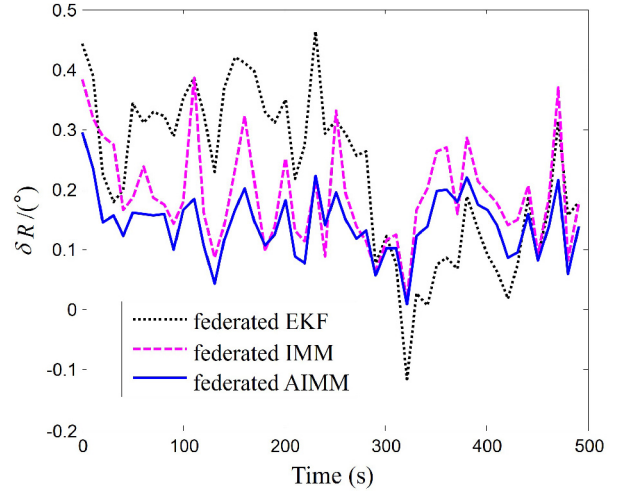
The trajectory and estimates using federated EKF, federated IMM and federated AIMM are shown in Fig. 4. This road test was performed for 500 seconds of continuous vehicle navigation. Figs. 5, 6 and 7 illustrate the performance of the three solutions in terms of attitude, velocity and position errors.

Fig. 5 depicts the attitude estimation errors. It can be seen that the pitch and roll estimation error decreased significantly at the beginning by all the three solutions. The yaw estimation error converges to the referenced value. However, the standard deviation (STD) of yaw estimation error is obviously larger than that of the pitch and roll estimation error. The results coincide with the observability analysis presented in [24]. The attitude tracking performance of federated IMM and federated AIMM is better than the federated EKF. The result indicates that the performance of the federated EKF depends highly on the magnitude of the measurement noise variance. On the other hand, the multiple model federated filters provide higher performance in estimating the yaw and are more stable than the federated extend Kalman filter when large errors exist in the measurement values.

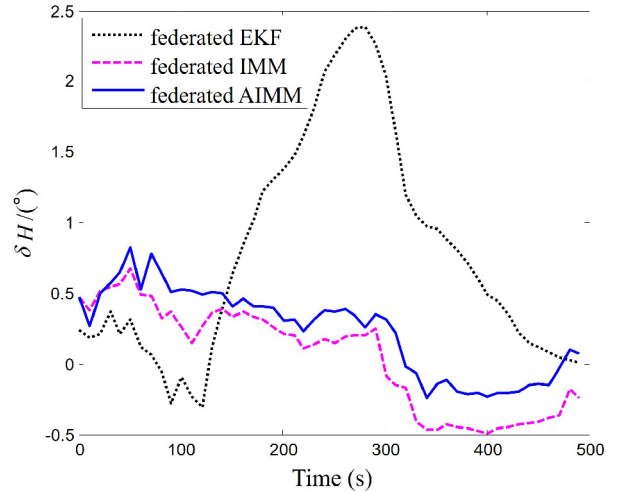
As can be seen from the Fig. 6, the horizontal velocity estimates converge to the value of reference by the three algorithms. The STDs of velocity estimation error by the federated EKF are larger than those by another two algorithms. The proposed federated AIMM filter and federated IMM filter have bounded estimate errors. It can be indi-



(a) The pitch angle error.

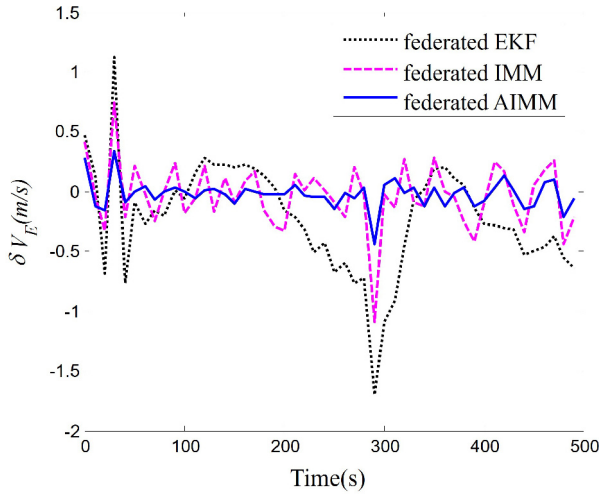


(b) The roll angle error.

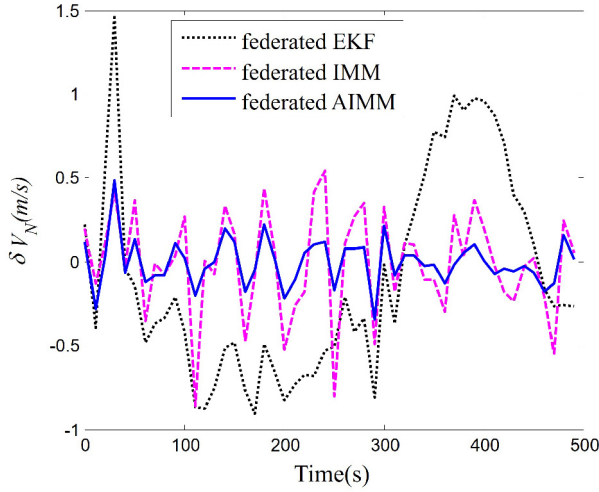


(c) The heading angle error.

Fig. 5. Attitude estimation errors.



(a) East velocity error.



(b) North velocity error.

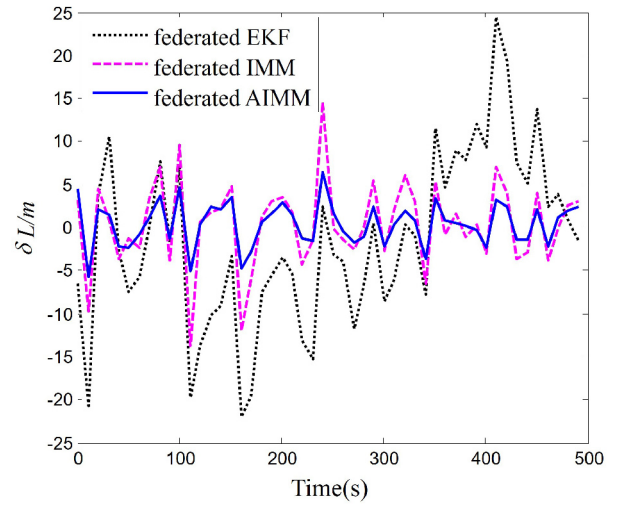
Fig. 6. Velocity estimation error curves.

cated that the multiple model based federated filters can provide a more robust estimate than single model based federated filters.

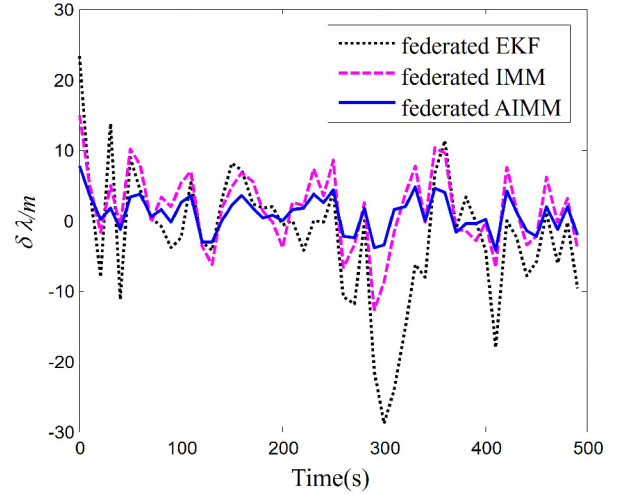
Fig. 7 shows the longitude and latitude estimation errors using the three solutions. The performances of longitude and latitude estimate of federated EKF, federated IMM filter and the proposed federated AIMM filter have similar features in comparison with the performances of the velocity estimate. For the performance comparison among the three solutions, the root-mean-square error (RMSE) of horizontal-axis position is defined as

$$RMSE_{pos} = \sqrt{\frac{1}{T} \sum_{t_k=1}^T (err_L(t_k)^2 + err_\lambda(t_k)^2)}, \quad (51)$$

where err_L and err_λ mean longitude error and latitude er-



(a) The latitude error.



(b) The longitude error.

Fig. 7. Longitude and latitude estimation error curves.

ror, respectively. T is the total navigation time of the vehicle. A total of five groups of data were post processed by federated EKF, federated IMM and federated AIMM. The RMSEs are plotted in Fig. 7.

As can be seen from Fig. 8, the horizontal-axis position RMSE estimated by federated EKF is the largest, and estimation by federated IMM is the second largest in RMSE. The federated AIMM has smallest RMSE. For the total five groups of test data, the federated EKF shows the average RMSE of 14.12 m, federated IMM shows 11.23 m and the proposed federated AIMM shows 8.55 m. We confirm that the multiple model based federated methods show better performance than federated EKF. As expected, the position error of the federated AIMM is smaller than that of the federated IMM. From Figs. 5 through 8, the position, velocity and attitude errors increase for the feder-

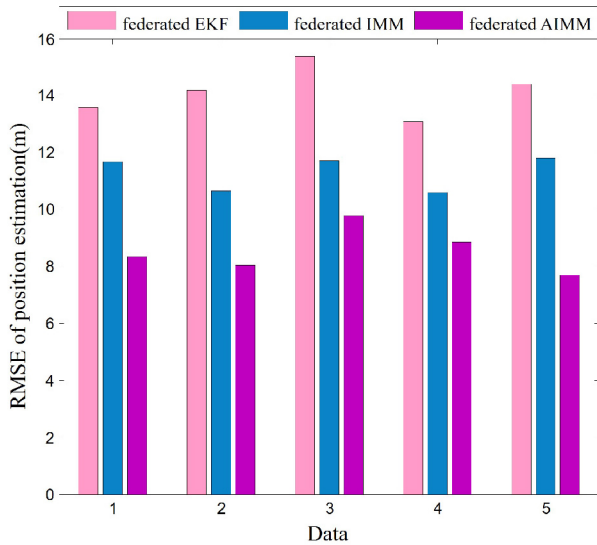


Fig. 8. RMSEs of five groups of test data.

ated EKF when the measurements have large position errors, but the error does not increase or increases by only a small amount for the two federated multiple model based filters. The process of innovation correction is utilized to get more accurate innovation for each parallel filter, so the tracking performance of the AIMM is better than that of the traditional IMM.

5. CONCLUSIONS

The major contribution of the proposed AIMM algorithm is the integration of inertial navigation system, global positioning system and odometer navigation system in multi-sensor data fusion formalism for land vehicle applications. It is utilized to solve the problem of parallel computing and fault-tolerant in the integrated navigation system. The performance of the proposed integrated navigation solution is demonstrated to be very competitive for vehicle navigation with low-cost sensors. This solution can be used in all environments including degraded GPS environments, which routinely occur in urban and rural canyons. The method has been verified on road tests in downtown scenarios. The results have been examined to verify the suitability and satisfactory performance of the proposed solution in downtown trajectories with degraded GPS and unusual maneuvers. The preliminary results showed the effectiveness of the proposed strategies.

REFERENCES

- [1] D. Huang, H. Leung, and N. El-Sheimy, "Expectation maximization based GPS/INS integration for land-vehicle navigation," *IEEE Trans. Aerospace and Electronic Systems*, vol. 43, no. 3, pp. 1168-1177, July 2007. [click]
- [2] A. Angrisano, S. Gaglione, and C. Gioia, "Performance assessment of aided global navigation satellite system for land navigation," *IET Radar, Sonar and Navigation*, vol. 7, no. 6, pp. 671-680, July 2013.
- [3] L. Wang and X. Cheng, "Algorithm of gaussian sum filter based on high-order UKF for dynamic state estimation," *International Journal of Control Automation and Systems*, vol. 13, no. 3, pp. 652-661, June 2015. [click]
- [4] M. Malleswaran, V. Vaidehi, and S. Irwin, "IMM-UKF-TFS model-based approach for intelligent navigation," *Journal of Navigation*, vol. 66, no. 6, pp. 859-877, July 2013. [click]
- [5] N. A. Carlson, "Federated filter for fault-tolerant integrated navigation systems," *Position Location and Navigation Symposium*, pp. 110-119, 1988.
- [6] M. J. Yu, "INS/GPS integration system using adaptive filter for estimating measurement noise variance," *IEEE Trans. Aerospace and Electronic Systems*, vol. 48, no. 2, pp. 1786-1792, April 2012. [click]
- [7] H. A. P. Blom and Y. Bar-Shalom, "The interacting multiple model algorithm for systems with Markovian switching coefficients," *IEEE Trans. Automatic Control*, vol. 33, no. 8, pp. 780-783, August 1988. [click]
- [8] X. R. Li, "Multiple-model estimation with variable structure. II. Model-set adaptation," *IEEE Trans. Automatic Control*, vol. 45, no. 11, pp. 2047-2060, November 2000. [click]
- [9] D. Dunne and T. Kirubarajan, "Multiple model multi-Bernoulli filters for manoeuvring targets," *IEEE Trans. Aerospace and Electronic Systems*, vol. 49, no. 4, pp. 2679-2692, October 2013. [click]
- [10] J. S. Evans and R. J. Evans, "Image-enhanced multiple model tracking," *Automatica*, vol. 35, no. 11, pp. 1769-1786, November 1999. [click]
- [11] N. Meskin, E. Naderi, and K. Khorasani, "A multiple model-based approach for fault diagnosis of jet engines," *IEEE Trans. Control Systems Technology*, vol. 21, no. 1, pp. 254-262, January 2013. [click]
- [12] P. Oliveira, "MMAE terrain reference navigation for underwater vehicles using PCA," *International Journal of Control*, vol. 80, no. 7, pp. 1008-1017, December 2007.
- [13] R. C. Zang, P. Y. Cui, H. T. Cui, and Y. Jin, "Integrated navigation algorithm based on IMM-UKF," *Control Theory and Applications*, vol. 24, no. 4, pp. 634-638, August 2007.
- [14] T. L. Xu, P. Y. Cui, and H. T. Cui, "Research on algorithm of adaptive interacting multiple model for integrated navigation system," *System Engineering and Electronics*, vol. 30, no. 11, pp. 2070-2074, November 2008.
- [15] Y. Liang, Q. Pan, D. H. Zhou, and H. C. Zhang, "Adaptive multiple model filter using IMM and STF," *Chinese Journal of Aeronautics*, vol. 13, no. 3, pp. 167-171, August 2000.
- [16] P. Quan, W. Peide, and Z. Hongren, "Innovation filter and its application to the IMM algorithm using Zhou model," *Proc. of International Conference on Circuits and Systems*, pp. 801-804, 1991.

- [17] S. Haykin and L. Liang, "Modified Kalman filtering," *IEEE Tans. Signal Processing*, vol. 27, no. 1, pp. 1239-1242, May 1994. [click]
- [18] J. H. Lee, K. C. Kwon, D. S. An, and D. S. Shim, "GPS spoofing detection using accelerometers and performance analysis with probability of detection," *International Journal of Control Automation and Systems*, vol. 13, no. 4, pp. 951-959, August 2015.
- [19] R. M. Roger, *Applied Mathematics in Integrated Navigation Systems*, American Institute of Aeronautics and Astronautics, Reston, 2003.
- [20] S. B. Kim, J. C. Bazin, H. K. Lee, and K. H. Choi, "Ground vehicle navigation in harsh urban conditions by integrating inertial navigation system, global positioning system, odometer and vision data," *IET Radar, Sonar and Navigation*, vol. 5, no. 8, pp. 814-823, November 2011. [click]
- [21] D. H. Titterton and J. L. Weston, *Strapdown Inertial Navigation Technology Second Edition*, American Institute of Aeronautics and Astronautics, Reston, 2004.
- [22] Y. Ma, J. Fang, W. Wang, and J. Li, "Decoupled observability analyses of error states in INS/GPS integration," *Journal of Navigation*, vol. 67, no. 3, pp. 473-494, May 2014. [click]
- [23] A. Ndjeng, D. Gruyer, S. Glaser, and A. Lambert, "Low cost IMU-Odometer-GPS ego localization for unusual maneuvers," *Information Fusion*, vol. 12, no. 4, pp. 264-274, January 2011.
- [24] S. Hong, H. L. Man, H. H. Chun, S. H. Kwon, and J. L. Speyer, "Observability of error states in GPS/INS integration," *IEEE Trans. Vehicular Technology*, vol. 54, no. 2, pp.731-743, March 2005. [click]



Lei Wang received the Ph.D. degree in control science and engineering from Southeast University, China, in 2015. He is currently a lecturer at Anhui Science and Technology University. His research interests include nonlinear filtering and estimation, sensor fusion, and statistical signal processing.



Shuangxi Li received his M.S. degree in electronics and communication engineering from Nanjing University of Posts and Telecommunications, China, in 2010. He is currently an associate professor at Anhui Science and Technology University. His research interests include nonlinear optimal control theory and nonlinear filtering.